

ESTIMATION OF COOLING FLUXES IN BOILING CONVECTION BY INVERSE HEAT CONDUCTION ON A ROTATING CYLINDER : FEASIBILITY STUDY

F. VOLLE¹, M. LÉBOUCHE, M. GRADECK and D. MAILLET

Laboratoire d'Énergétique et de Mécanique Théorique et Appliquée - UMR 7563 CNRS - Institut National Polytechnique de Lorraine - Université Henri Poincaré Nancy 1, France

¹ e-mail : fabien.volle@ensem.inpl-nancy.fr

Abstract - A theoretical study of heat exchange during the cooling of a rotating cylinder by an impinging jet is carried out. The temperature field is bidimensional - the longitudinal heat conduction being neglected - and is obtained by solving the heat equation using Laplace and Fourier transforms. In order to assess the external heat flux condition, an inverse method using simulated temperature measurements inside the cylinder is carried out. The results of this study show that the method is reliable, in spite of a non-negligible influence of the measurement errors.

1. INTRODUCTION

Impinging jets are very effective means for cooling solid media : a cold fluid jet that impacts a hot surface vaporizes partly. By this technique, it is possible to locally extract very important heat fluxes, the latent heat associated with phase change of the working fluid being used to yield higher heat transfer coefficients.

This kind of techniques concerns many engineering applications : cooling of increasingly powerful chips in electronics, [11], cooling of tools during machining, [4,5], ... In order to avoid any heterogeneity in the resulting properties that can stem from rewatering or from nonuniform temperature, models are necessary for the prediction of water cooling and for its local control. We will focus here on the problem of the control of the thermal path taken by a moving metal part.

A transient two-dimensional inverse method - based on singular value decomposition and a function specification method - will be used to estimate wall heat flux in liquid jet cooling of a moving solid. Simulated inversion on a noised signal are thus presented. Future work will be concerned to the use of experimental data - the experimental set-up being in construction - in order to assess real cooling fluxes.

2. DIRECT HEAT TRANSFER PROBLEM

A rotating metal cylinder (angular velocity ω in the direct orientation of Figure 1) of length l , is composed of two layers of radii r_1 and r_2 as shown in Figure 1. A uniform and time-constant surface heat source $P(W)$ can be dissipated by Joule heating through electrical heating at the interface radius r_1 . In practice, it will be implemented through three electrical wires inserted into grooves machined in the internal surface of the external cylinder. The length of the cylinder is assumed to be a lot larger than the external radius in order to consider the axial heat transfer as negligible. The values of all the parameters that will be used in the simulations are given in Table 1.

Table 1 : Parameters used in the study.

Parameter	Value
λ	90,7 W.m ⁻¹ .K ⁻¹
ρc	3.919.520 J.m ⁻³
r_1, r_2, l	0,049 m, 0,0875 m, 0,4 m
P, ω	6000 W, 6 rad.s ⁻¹
h, T_e	100 W.m ⁻² .K ⁻¹ , 20 °C

Neglecting axial heat conduction, the temperature T_i in each domain i ($i = 1, 2$), in a non-moving laboratory coordinates system, is solution of the heat equation associated with its initial, boundary and periodicity conditions :

$$\frac{\partial^2 T_i}{\partial r^2} + \frac{1}{r} \frac{\partial T_i}{\partial r} + \frac{1}{r^2} \frac{\partial^2 T_i}{\partial \gamma^2} - \frac{\omega}{a} \frac{\partial T_i}{\partial \gamma} = \frac{1}{a} \frac{\partial T_i}{\partial t} \quad (1)$$

where a is the material (Nickel) thermal diffusivity of both layers, defined by $a = \frac{\lambda}{\rho C_p}$.

The boundary and interface conditions are the following :

$$\begin{cases} -\lambda \frac{\partial T_2}{\partial r}(r = r_2, \gamma) = h(\gamma)[T_2 - T_e] & ; & \frac{\partial T_1}{\partial r}(r = 0) = 0 & ; & T_i(r, \gamma + 2\pi) = T_i(r, \gamma) \\ \frac{P}{2\pi r_1 l} - \lambda \frac{\partial T_1}{\partial r}(r = r_1, \gamma) = -\lambda \frac{\partial T_2}{\partial r}(r = r_1, \gamma) & ; & & & T_1(r = r_1, \gamma) = T_2(r = r_1, \gamma) \end{cases} \quad (2)$$

the initial condition being :

$$T_i(r, \gamma, t = 0) = T^{SS}(r) \quad (3)$$

The first boundary condition does not allow the use of the method of separation of variables due to the nonconstant value of coefficient $h(\gamma)$. In order to overcome this difficulty, it is possible to use a variable flux density condition φ on the outer radius instead :

$$-\lambda \frac{\partial T_2}{\partial r}(r = r_2, \gamma) = \varphi_2(\gamma) \quad (4)$$

The direct problem that is considered can then be solved by expressing temperature T in terms of function $\varphi_2(\gamma)$. It corresponds to a two-fold thermal excitation :

- starting from thermal equilibrium at temperature T_e (equal to air temperature), the rotating cylinder is heated at $r = r_1$ with a uniform surface heat source $P(W)$ that does not vary with time. The heat is dissipated by convection (and radiation) at $r = r_2$ through a uniform heat transfer coefficient h . The considered steady-state heat transfer T^{SS} (see Figure 1) is solution of the system (where subscript i designates temperature T in the central layer ($0 \leq r < r_1$; $i = 1$) and in the outer layer ($r_1 < r \leq r_2$; $i = 2$))

$$\frac{d^2 T_i}{dr^2} + \frac{1}{r} \frac{dT_i}{dr} = 0 \quad (5)$$

$$\begin{cases} -\lambda \frac{dT_2}{dr}(r = r_2) = h[T_2 - T_e] & ; & T_1(r = r_1) = T_2(r = r_1) \\ \frac{P}{2\pi r_1 l} - \lambda \frac{dT_1}{dr}(r = r_1) = -\lambda \frac{dT_2}{dr}(r = r_1) & ; & -\lambda \frac{dT_1}{dr}(r = 0) = 0 \end{cases} \quad (6)$$

hence

$$\begin{cases} T^{SS}(r \leq r_1) = T_e + P \left(\frac{1}{2\pi r_2 l h} + \frac{1}{2\pi \lambda l} \ln\left(\frac{r_2}{r_1}\right) \right) = T_c \\ T^{SS}(r \geq r_1) = T_c - \frac{P}{2\pi \lambda l} \ln\left(\frac{r}{r_1}\right) \end{cases} \quad (7)$$

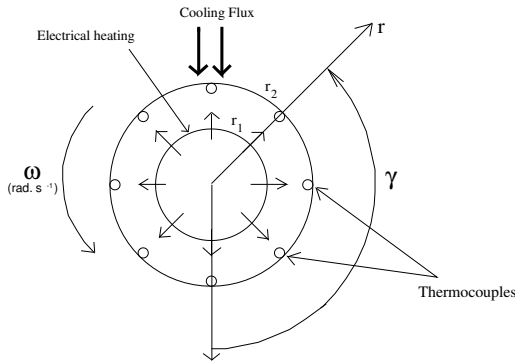


Figure 1 : Model geometry and steady-state temperature distribution.

- at time $t = 0$, a water jet centered at $\gamma = \pi$ impinges on the cylinder and creates a moving liquid film at the cylinder surface : the resulting surface heat flux at $r = r_2$ in the laboratory frame is $\varphi_2(\gamma, t)$. This transient regime is considered until a new equilibrium is reached for $P = 2\pi r_2 l \varphi_{2\text{ave}}(\infty)$, where $\varphi_{2\text{ave}}$ is the angular average of φ_2 . The resulting transient temperature field in the cylinder T^t is the sum of the solutions of three problems :

$$T^t(r, \gamma, t) = T^{\text{relax}}(r, t) + T^{\text{adia}}(r, t) + T^{\text{cool}}(r, \gamma, t) \quad (8)$$

- T^{relax} (resp. T^{adia}) is the axisymmetrical 1D transient temperature field that results from the natural relaxation of the initial $T^{SS}(r)$ field (resp. produced by internal heating P at radius r_1) inside the cylinder that is now insulated (adiabatic boundary at $r = r_2 : h = 0$) with internal heating P (resp. the initial temperature) being equal to zero. These two fields are described by the equation

$$\frac{d^2 T_i}{dr^2} + \frac{1}{r} \frac{dT_i}{dr} = \frac{1}{a} \frac{dT_i}{dt} \quad (9)$$

the initial and boundary conditions being

$$\text{for } T^{relax} : \begin{cases} -\lambda \frac{dT_2}{dr}(r = r_2) = 0 & ; & -\lambda \frac{dT_1}{dr}(r = 0) = 0 & ; & T_i(r, t = 0) = T^{SS}(r) \\ -\lambda \frac{dT_1}{dr}(r = r_1) = -\lambda \frac{dT_2}{dr}(r = r_1) & ; & & ; & T_1(r = r_1) = T_2(r = r_1) \end{cases} \quad (10)$$

$$\text{for } T^{adia} : \begin{cases} -\lambda \frac{dT_2}{dr}(r = r_2) = 0 & ; & -\lambda \frac{dT_1}{dr}(r = 0) = 0 & ; & T_i(r, t = 0) = 0 \\ \frac{P}{2\pi r_1 l} - \lambda \frac{dT_1}{dr}(r = r_1) = -\lambda \frac{dT_2}{dr}(r = r_1) & ; & & ; & T_1(r = r_1) = T_2(r = r_1) \end{cases} \quad (11)$$

Applying the Laplace transform to the time variable t that is replaced by Laplace parameter p

$$L[T(r, t)] = \bar{T}(r, p) = \int_0^{+\infty} T(r, t) \exp(-pt) dt \quad (12)$$

then solving the obtained equations, we have with $\alpha = \sqrt{\frac{p}{a}}$:

$$\bar{T}_1^{relax}(r, p) = -\frac{P}{2\pi\lambda l p} \left\{ \left[K_0(\alpha r_1) + \frac{I_0(\alpha r_1)}{I_1(\alpha r_2)} K_1(\alpha r_2) \right] - \frac{1}{\alpha r_2} \frac{1}{I_1(\alpha r_2)} \right\} I_0(\alpha r) + \frac{T^{SS}(r)}{p} \quad (13)$$

$$\bar{T}_2^{relax}(r, p) = -\frac{P}{2\pi\lambda l p} \left\{ \left[K_0(\alpha r) + \frac{K_1(\alpha r_2)}{I_1(\alpha r_2)} I_0(\alpha r) \right] I_0(\alpha r_1) - \frac{1}{\alpha r_2} \frac{I_0(\alpha r)}{I_1(\alpha r_2)} \right\} + \frac{T^{SS}(r)}{p} \quad (14)$$

and

$$\bar{T}_1^{adia}(r, p) = \frac{P r_1}{\lambda p} \left[K_0(\alpha r_1) + \frac{I_0(\alpha r_1)}{I_1(\alpha r_2)} K_1(\alpha r_2) \right] I_0(\alpha r) \quad (15)$$

$$\bar{T}_2^{adia}(r, p) = \frac{P r_1}{\lambda p} \left[K_0(\alpha r) + \frac{K_1(\alpha r_2)}{I_1(\alpha r_2)} I_0(\alpha r) \right] I_0(\alpha r_1) \quad (16)$$

Return in the time domain is made numerically using Stehfest's algorithm, [9,10] :

$$T_i(r, t) = \frac{\ln 2}{t} \sum_{j=1}^N V_j \bar{T}_i \left(r, p = \frac{j \ln 2}{t} \right) \quad \text{with } N=10 \text{ in our case} \quad (17)$$

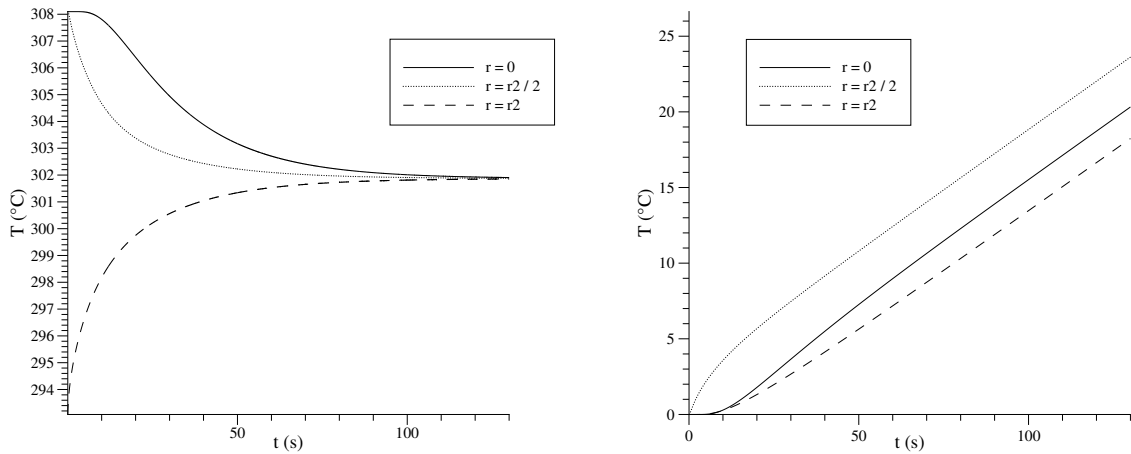


Figure 2 : Temperature distribution during relaxation (left) and adiabatic heating (right) regimes.

- T^{cool} is the 2D transient temperature field that is produced by surface jet cooling $\varphi_2(\gamma, t)$, without any internal heating ($P = 0$) and starting from an initial zero temperature field.

2.1. Study of the jet cooling regime

Axial heat conduction being neglected and the cylinder being considered as a monolayer cylinder, temperature is solution of the following equation in a non-moving laboratory coordinates system :

$$\frac{\partial^2 T}{\partial r^2} + \frac{1}{r} \frac{\partial T}{\partial r} + \frac{1}{r^2} \frac{\partial^2 T}{\partial \gamma^2} - \frac{\omega}{a} \frac{\partial T}{\partial \gamma} = \frac{1}{a} \frac{\partial T}{\partial t} \quad (18)$$

the associated boundary conditions being :

$$\begin{cases} T(r, \gamma + 2\pi) = T(r, \gamma) \text{ (periodicity conditions)} \\ -\lambda \frac{\partial T}{\partial r}(r = r_2, \gamma) = \varphi_2(\gamma, t) \quad ; \quad \frac{\partial T}{\partial r}(r = 0) = 0 \end{cases} \quad (19)$$

and the initial condition :

$$T(r, \gamma, t = 0) = 0 \quad (20)$$

The considered cooling flux φ_2 , that is shown in Figure 3, is assumed to be gaussian and is given by

$$\varphi_2(\gamma, t) = K_t e^{-\frac{1}{2} \left(\frac{\gamma - \pi}{\sigma_c} \right)^2} e^{-t/t_c} + \frac{P}{2\pi r_2 l} \quad (21)$$

with $K_t = 10^6 \text{ W} \cdot \text{m}^{-2}$ and $\sigma_c = 0.456 \text{ rad}$ (which corresponds to the angular thickness of the jet). The second term in this equation allows a steady-state asymptotic solution ($t \rightarrow \infty$) equal to T_e for T^t (see eqn.(8)).

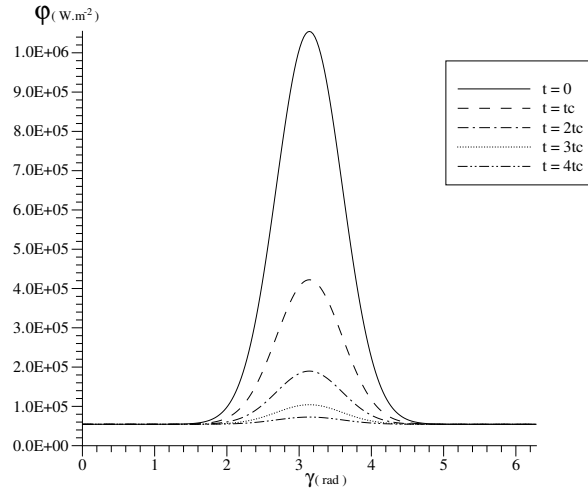


Figure 3 : Distribution of the cooling flux φ_2 with respect to time.

The periodicity conditions relative to the γ -coordinate allow us to use the Fourier transformation (superscript \sim) in the γ -direction associated with the Laplace transformation (superscript $-$) applied to the time variable :

$$\tilde{\tilde{T}}(r, n, p) = \int_0^\infty \int_0^{2\pi} T(r, \gamma, t) \exp(-j n \gamma) \exp(-p t) d\gamma dt \quad (22)$$

The double transform of the radial heat flux density $\varphi = -\lambda \frac{\partial T}{\partial r}$ is linked to the transformed temperature by

$$\tilde{\tilde{\varphi}}(r, n, p) = \int_0^\infty \int_0^{2\pi} \left(-\lambda \frac{\partial T}{\partial r} \right) \exp(-j n \gamma) \exp(-p t) d\gamma dt = -\lambda \frac{d\tilde{\tilde{T}}}{dr} \quad (23)$$

Applying this transformation to eqn.(18), then making a double integration by parts that takes into account the boundary as well as the periodicity and initial conditions yields :

$$\frac{d^2 \tilde{\tilde{T}}}{dr^2} + \frac{1}{r} \frac{d\tilde{\tilde{T}}}{dr} - \left(\frac{n^2}{r^2} + \frac{p}{a} + j n \frac{\omega}{a} \right) \tilde{\tilde{T}} = 0 \quad (24)$$

with boundary conditions :

$$\begin{cases} \frac{d\tilde{T}}{dr}(r = 0, n, p) = 0 \\ -\lambda \frac{d\tilde{T}}{dr}(r = r_2, n, p) = \tilde{\varphi}_2(n, p) \end{cases} \quad (25)$$

The general solution for eqn.(24) uses the modified Bessel functions :

$$\tilde{T}(r, n, p) = a_n I_n(\alpha_n r) + b_n K_n(\alpha_n r), \quad \text{with } \alpha_n = \sqrt{\frac{p + j n \omega}{a}} \quad (26)$$

The solution of system (24)-(25) is :

$$\tilde{T}(r, n, p) = -\frac{1}{\lambda} \frac{I_n(\alpha_n r)}{\alpha_n I_n'(\alpha_n r_2)} \tilde{\varphi}_2(n, p) \quad (27)$$

with $I_n'(x)$ the derivative of $I_n(x)$ being calculated as :

$$I_n'(\alpha r_2) = \alpha I_{n-1}(\alpha r_2) - \frac{n}{\alpha r_2} I_n(\alpha r_2) \quad (28)$$

The shift property of the Laplace transform (operator $L(\cdot)$) can be written as $F(p+K) = L\left[exp(-K t) f(t)\right]$

- where $F(p) = L\left[f(t)\right]$ - and can be applied to eqn.(27) with $K = j n \omega$, which gives the following expression for the n^{th} harmonic of temperature in the time domain using a convolution product :

$$\tilde{T}(r, n, t) = -\frac{1}{\lambda} \int_0^t \left[\tilde{\varphi}_2(n, \tau) \right] \left[e^{-j n \omega (t-\tau)} Z_n(r, t - \tau) \right] d\tau = \tilde{T}_n \quad (29)$$

with

$$\bar{Z}_n(r, p) = \frac{I_n\left(\sqrt{\frac{p}{a}} r\right)}{\sqrt{\frac{p}{a}} I_n'\left(\sqrt{\frac{p}{a}} r_2\right)} = F(r, p) \quad (30)$$

Return to the original space domain is given by the following expression :

$$T^{cool}(r, \gamma, t) = \frac{\tilde{T}_0}{2\pi} + \sum_{n=1}^{\infty} \left[\frac{\tilde{T}_n}{2\pi} e^{jn\gamma} \right] + \sum_{n=1}^{\infty} \left[\frac{\tilde{T}_n^*}{2\pi} e^{-jn\gamma} \right] \quad (31)$$

where superscript `*` designates the complex conjugate.

Hence :

$$T^{cool}(r, \gamma, t) = \frac{\tilde{T}_0}{2\pi} + \frac{1}{\pi} \sum_{n=1}^{\infty} \left[Re(\tilde{T}_n) \cos(n\gamma) - Im(\tilde{T}_n) \sin(n\gamma) \right] \quad (32)$$

2.2. Results for the direct problem

Measurements are made through N_{TC} thermocouples that are embedded in the moving cylinder at radius $r = r_2$. At $t = 0$, when the jet impinges the cylinder, the first thermocouple is at angle $\gamma_1(0) = \gamma_{ref}$. At the same time, thermocouple number m ($m = 1$ to N_{TC}) is at angle $\gamma'_m = \gamma_m(0) = \gamma_{ref} + (m - 1)\Delta\gamma$, where $\Delta\gamma = 2\pi/N_{TC}$. At later time, angle $\gamma_m(t)$ is given by

$$\gamma_m(t) = \gamma'_m + \omega t \quad (33)$$

The observed temperature for this thermocouple $T_m^t(t) = T^t(r_2, \gamma_m(t), t)$, see eqn.(8), is calculated through a numerical quadrature (trapezoidal rule) with a $\Delta t = 0.1$ s time step. Moreover, because of the unbounded behavior of $Z_n(r_2, t)$ as t goes to zero, this function is approximated by

$$\check{Z}_n(r_2, t) = \sqrt{\frac{a}{\pi t}} + \frac{1}{2} \frac{a}{r_2} \quad \text{for } t < t_{lim} = i_{lim} \Delta t. \quad (34)$$

Excitation $\varphi_2(\gamma_m(t), t)$ for $m = 1$ and $\gamma_{ref} = \pi$, given by equation (21), as well as temperature responses $T^t(t)$ and $T^{cool}(t)$, are plotted in Figure 6 for $t_c = 1$ s. A total number of $N_H = 12$ harmonics have been used for the truncation of eqn.(32). Indeed, since the total number of harmonics depends on the space shape of heat flux φ_2 , the optimal value for the studied test case is $N_H = 12$ for $N_{TC} = 24$ thermocouples, which corresponds to Shannon's sampling theorem.

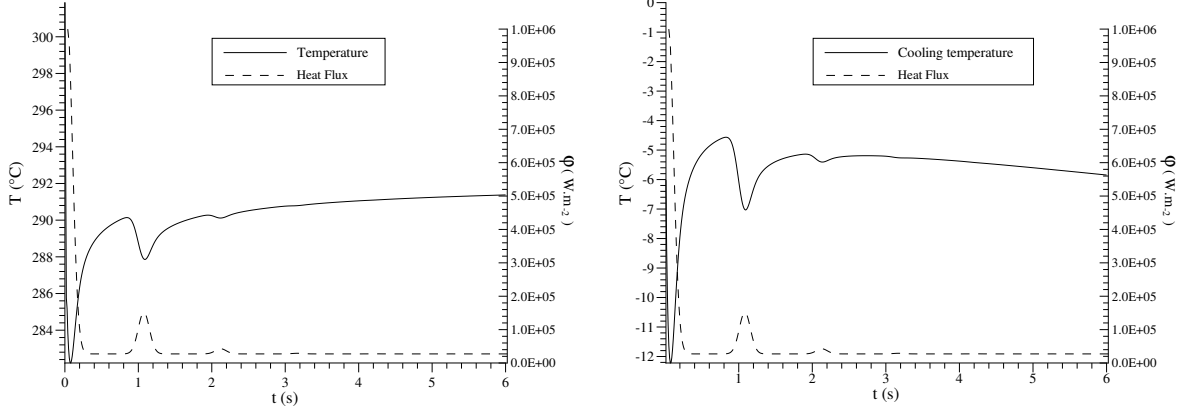


Figure 4 : Variations of $T^t(t)$ and $T^{cool}(t)$ for the first thermocouple at $r = r_2$ (with $\gamma_{ref} = \pi$).

3. INVERSE PROBLEM

The inverse problem consists in estimating the surface heat flux φ_2 starting from transient measurements of N_{TC} temperature sensors ($N_{TC} = 24$ thermocouples) located at the boundary $r = r_2$. All other quantities appearing in the formulation of the physical problem are assumed to be exactly known, but the measurements may contain random errors. We consider here only the cooling component $T = T^{cool}$. Let's consider eqn.(29) :

$$\tilde{T}(r, n, t) = -\frac{1}{\lambda} \int_0^t \left[\tilde{\varphi}_2(n, \tau) \right] \left[e^{-j n \omega (t-\tau)} Z_n(r, t-\tau) \right] d\tau \quad (35)$$

As $Z_n \rightarrow \infty$ when $t \rightarrow \tau$, we use an asymptotic behavior $\check{Z}_n(r_2, t-\tau)$ for $Z_n(r, t-\tau)$ and we obtain

$$\begin{aligned} \tilde{T}(r, n, t) = & -\frac{1}{\lambda} \left[\int_0^{t-t_{lim}} \tilde{\varphi}_2(n, \tau) e^{-j n \omega (t-\tau)} Z_n(r, t-\tau) d\tau \right. \\ & \left. + \int_{t-t_{lim}}^t \tilde{\varphi}_2(n, \tau) e^{-j n \omega (t-\tau)} \left(\sqrt{\frac{a}{\pi(t-\tau)}} + \frac{1}{2} \frac{a}{r_2} \right) d\tau \right] \end{aligned} \quad (36)$$

In practice, we evaluate this expression using a piecewise constant function φ_2 :

$$\varphi_2(\gamma, t) = \varphi_{2k}(\gamma) \quad \text{for } t_k \leq t \leq t_{k+1} \quad (37)$$

with $t_k = k\Delta t$ and $k \geq 0$, where Δt is both a discretization time step for φ_2 and a calculation time step for temperature T .

It yields for $t_i = i\Delta t$ ($i \geq 2$) and with $t_0 = 0$ and $\tilde{\varphi}_{2nk} = \int_0^{2\pi} \varphi_{2k}(\gamma) e^{-j n \gamma} d\gamma$:

$$\begin{aligned} \tilde{T}(r, n, t_i) = & -\frac{1}{\lambda} \left[\sum_{k=0}^{i-2} \tilde{\varphi}_{2nk} \int_{t_k}^{t_{k+1}} e^{-j n \omega (t_i-\tau)} Z_n(r, t_i-\tau) d\tau \right. \\ & \left. + \tilde{\varphi}_{2n(i-1)} \int_{t_{i-1}}^{t_i} e^{-j n \omega (t_i-\tau)} \left(\sqrt{\frac{a}{\pi(t_i-\tau)}} + \frac{1}{2} \frac{a}{r_2} \right) d\tau \right] \end{aligned} \quad (38)$$

hence

$$\tilde{T}(r, n, t_i) = \sum_{k=0}^{i-1} X_{i,k+1} \tilde{\varphi}_{2nk} \quad (39)$$

where the coefficients $X_{i,k+1}$ are :

$$X_{i,k+1} = -\frac{1}{\lambda} \int_{t_k}^{t_{k+1}} e^{-j n \omega (t_i-\tau)} L^{-1} \left[\frac{I_n \left(\sqrt{\frac{E}{a}} r \right)}{\sqrt{\frac{E}{a}} I_n' \left(\sqrt{\frac{E}{a}} r_2 \right)} \right]_{t_i-\tau} d\tau \quad \text{if } k < i - i_{lim} \quad (40)$$

and

$$X_{i,k+1} = -\frac{1}{\lambda} \int_{t_k}^{t_{k+1}} e^{-jn\omega(t_i-\tau)} \left(\sqrt{\frac{a}{\pi(t_i-\tau)}} + \frac{1}{2} \frac{a}{r_2} \right) d\tau \quad \text{if } k \geq i - i_{lim} \quad (41)$$

This yields in a matrix form

$$\tilde{T}(r, n) = \begin{pmatrix} \tilde{T}(r, n, t_1) \\ \vdots \\ \tilde{T}(r, n, t_i) \end{pmatrix} = \begin{pmatrix} X_{11} & \dots & 0 \\ \vdots & \ddots & \vdots \\ X_{i1} & \dots & X_{ii} \end{pmatrix}_n \begin{pmatrix} \tilde{\varphi}_{2n,0} \\ \vdots \\ \tilde{\varphi}_{2n,i-1} \end{pmatrix} = X_n(r) \tilde{\varphi}_{2n} \quad (42)$$

where matrix \mathbf{X} is the *sensitivity matrix*, which defines the relationship between a change in the surface heat flux and the corresponding change in the computed temperature response \tilde{T}_n .

An excitation φ_2 has been generated according to (21) and discretized by time averaging according to (37). $\tilde{\varphi}_{2nk}$ has then been calculated through numerical quadrature and direct solution of (42) for $r = r_2$ yields simulated values of $T_m(t)$ through (32).

Starting from $T_m(t)$, one gets a simulated experimental signal for thermocouple m

$$Y_m(t_i) = T_m(t_i) + \epsilon_{mi} \quad (43)$$

where ϵ_{mi} ($m = 1$ to N_{TC} , $i = 1$ to i_f) is an uncorrelated, zero mean and identically distributed normal noise of constant standard deviation σ .

Then, experimental Fourier transforms of temperatures Y_m are calculated through :

$$\tilde{Y}_{n,i} = \sum_{m=1}^{N_{TC}} Y_m(t_i) e^{-jn\gamma_m(t_i)} \Delta\gamma \quad (44)$$

The vector φ_{2n} is finally estimated from transforms of measured temperature \tilde{Y}_n using the estimator of the ordinary least squares, [1],

$$\hat{\varphi}_{2n} = (X_n^t X_n)^{-1} X_n^t \tilde{Y}_n \quad (45)$$

with $\tilde{Y}_n = [\tilde{Y}_{n,1} \dots \tilde{Y}_{n,i}]^t$.

Return to the original space domain is made by applying the inverse Fourier transform.

Exact and recalculated temperatures as well as exact and estimated cooling heat fluxes are plotted in Figure 5 for a noise having a standard deviation $\sigma = 0.1^\circ\text{C}$ and in Figure 6 for a noise having a standard deviation $\sigma = 0.5^\circ\text{C}$.

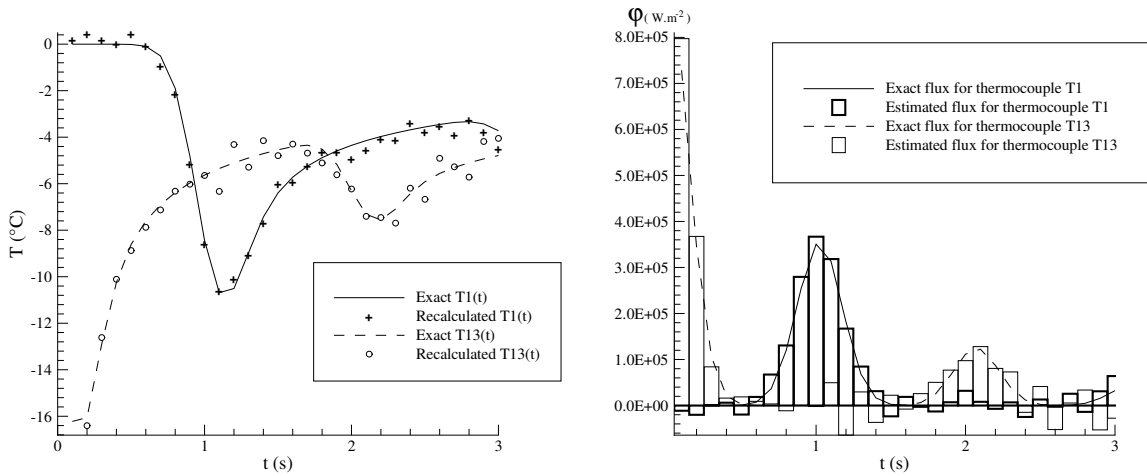


Figure 5 : Exact and estimated temperatures and flux for $\gamma_{ref} = 0$ and $\gamma_{ref} = \pi$ with $\sigma = 0.1^\circ\text{C}$.

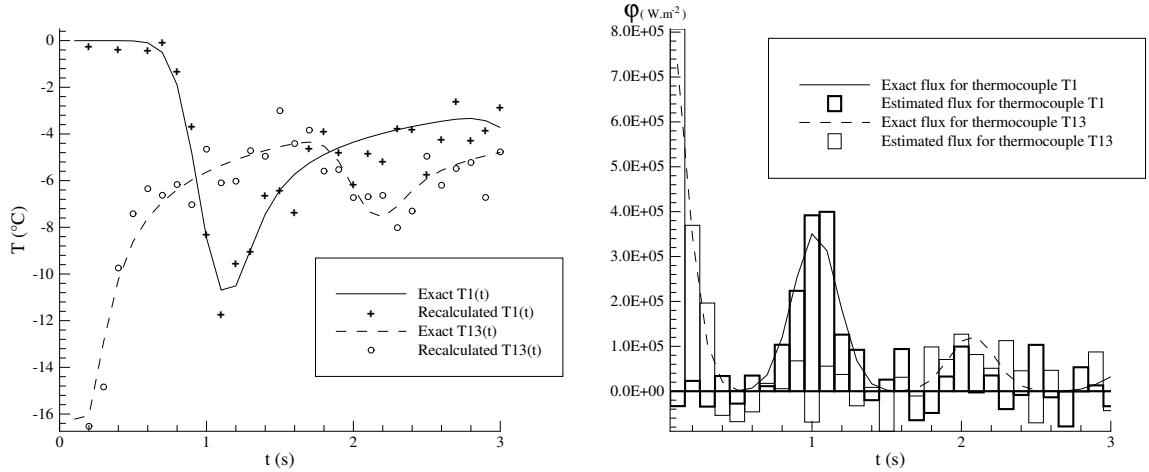


Figure 6 : Exact and estimated temperatures and flux for $\gamma_{ref} = 0$ and $\gamma_{ref} = \pi$ with $\sigma = 0.5^\circ\text{C}$.

In each case, we have considered thermocouples T_1 and T_{13} , which correspond respectively to $\gamma_{ref} = 0$ (opposite side of the jet at $t = 0$) and $\gamma_{ref} = \pi$ (under the jet at $t = 0$).

We can see that our inversion problem is quite well-posed : a five fold increase of the noise standard deviation (from 0.1 to 0.5°C) does not destabilize the reconstructed flux and yields quite good temperature residuals. These residuals are higher for times when the thermocouples are far from the jet. We can notice that a finer time step for the flux (0.01 s instead of 0.1 s, for $\sigma = 0.5^\circ\text{C}$) leads to an unstable inversion (not shown here), which shows that the flux parametrization step constitutes the first regularization factor.

4. CONCLUSION

An analytical solution is obtained for the two-dimensional transient temperature response of a finite-length rotating heated cylinder subjected to a known but time-dependent and not uniform cooling heat flux at its surface. This solution, based on the idea of Laplace and Fourier transforms, is obtained by solving the heat equation and is explicitly given using series expansions and modified Bessel functions. Using the thermophysical properties of Nickel, the variations of transient temperature inside the sample is computed and presented for demonstration purpose.

Right now, in our first simulations, it has been shown that a whole time domain inversion technique applied on experimental Fourier angular transform of measured temperatures (which corresponds to a space Singular Value Decomposition, [6,8], and stems directly from the quadrupole method used in a transformed space, [3,7]) allows to recover the surface heat flux, which is possible as long as noise is small enough. A more powerful time inversion technique using Beck's future time steps, [2], will be implemented in the near future, and an experimental set-up based on this study - see Figure 7 below - is about to be used.

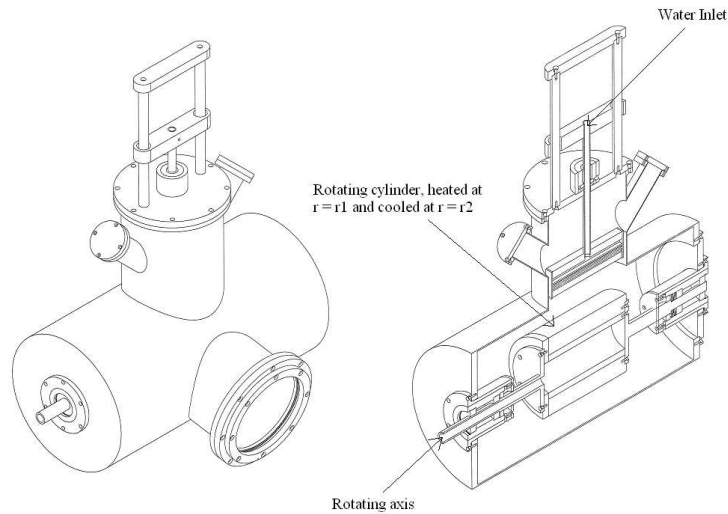


Figure 7 : Experimental set-up.

REFERENCES

1. J.-V. Beck and K.J. Arnold, *Parameter Estimation in Engineering and Science*, John Wiley and Sons, New-York, 1977.
2. J.-V. Beck, B. Blackwell and C.-R. St-Clair Jr., *Inverse Heat Conduction - Ill-Posed Problems*, John Wiley and Sons, New-York, 1985.
3. Ph. Leturcq, J.M. Dorkel, F.E. Ratolojanarhary and S. Tounsi, A two-port network formalism for 3D heat conduction analysis in multilayered media. *Int. J. Heat Mass Transfer* (1993) **36**(9), 2317-2326.
4. X. Li, Study of the jet-flow rate of cooling in machining Part 1. Theoretical analysis. *J. Mat. Proc. Tech.* (1996) **62**, 149-156.
5. X. Li, Study of the jet-flow rate of cooling in machining Part 2. Simulation analysis. *J. Mat. Proc. Tech.* (1996) **62**, 157-165.
6. P. Linz, A new numerical method for ill-posed problems. *Inverse Problems* (1994) **10**(1), L1-L6.
7. D. Maillet, S. André, J.-C. Batsale, A. Degiovanni and C. Moyne, *Thermal Quadrupoles : Solving the Heat Equation through Integral Transforms*, John Wiley and Sons, UK, 2000.
8. D. Maillet, A. Degiovanni and S. André, Estimation of a Space-Varying Heat Transfer Coefficient or Interface Resistance by Inverse Conduction, *Proceedings of the 23rd International Conference on Thermal Conductivity*, Tecnomac Pub.Co, Lancaster, Pennsylvania, 1996, pp.72-84.
9. H. Stehfest, Algorithm 368 : Numerical inversion of Laplace transforms. *Commun. ACM* (1970) **13**(1), 47-49.
10. H. Stehfest, Remark on algorithm 368 : Numerical inversion of Laplace transforms. *Commun. ACM* (1970) **13**(10), 624.
11. E.N. Wang, L. Zhang, L. Jiang, J.-M. Koo, J. Maveety, E. Sanchez, K.E. Goodson and T.W. Kenny, Micromachined jets for liquid impingement cooling of VLSI chips. *J. Microelectromech. Syst.* (2004) **13**(5), 833-842.